Pramana – J. Phys. (2018) 91:41
https://doi.org/10.1007/s12043-018-1624-z

Fabrication and photoresponse of n-WS_2/p-$V_{0.25}W_{0.75}Se_2$ van der Waals heterojunction

PRATIK PATANIYA[1,*], G K SOLANKI[1,*], CHETAN K ZANKAT[1], MOHIT TANNARANA[1], C K SUMESH[2], K D PATEL[1] and V M PATHAK[1]

[1]Department of Physics, Sardar Patel University, Vallabh Vidyanagar, Anand 388120, India
[2]Department of Physical Sciences, P.D. Patel Institute of Applied Sciences, Charusat, Changa 388 421, India
*Corresponding authors. E-mail: pm.pataniya9991@gmail.com; solankigunvant@yahoo.co.in

MS received 2 September 2017; revised 9 February 2018; accepted 13 March 2018; published online 1 August 2018

Abstract. Transition metal dichalcogenides (TMDCs) have shown tremendous potential for application in the field of optoelectronics owing to their extraordinary characteristics. The $WS_2/V_{0.25}W_{0.75}Se_2$ van der Waals heterostructure was fabricated by layer transfer technique and its I–V characteristic was measured at room temperature. The fabricated pn-junction heterostructure shows obvious current rectification with a rectification ratio of ∼39 at ±1 V. The heterostructure was analysed in the dark and under polychromatic illumination. The noticeable rise in reverse current is observed at higher intensity of illumination. The photocurrent and photoresponsivity are found to be enhanced as intensity and bias voltage are increased. The higher value of the ideality factor of ∼2 is attributed to the inhomogeneity of the heterojunction.

Keywords. van der Waals heterojunction; photoresponse; responsivity.

PACS Nos 07.07.Df; 61.72.Ww; 61.82.Fk

1. Introduction

Recently, layered materials including graphene and transition metal dichalcogenides (TMDCs) have attracted considerable attention in the field of electronics, optoelectronics and photonics [1–11]. The TMDCs with the generalised formula MX_2 (where M is a transition metal atom and X is a chalcogen atom) are composed of two-dimensional trilayer X–M–X sandwich structures. The M atom plane is in the middle of the two hexagonal X atom planes. These MX_2 sheets are weakly bonded together by van der Waal bonding to form crystals and hence the layers can easily be separated by mechanical or chemical exfoliation [12–15]. Besides this, the TMDCs exhibit layer-dependent properties, e.g. the indirect band gap of bulk materials converts into the direct band gap when the dimensions are confined to the monolayer [16–18]. The important members of the TMDC family, WS_2 and WSe_2, have found great applications due to their unique electrical and optical properties. The band gap of 1–1.5 eV and excitonic mechanism make these materials ideal for photovoltaics and photoconduction [11,19]. Moreover, the TMDCs have attracted huge attention due to their unique electrical properties including high mobility, conductivity, carrier concentration, etc. The properties of these semiconductors can also be tailored by doping or substitution or the intercalation process and semiconducting nature can also be changed [20–31]. Hyun Seok Lee and coworkers have reported the transformation from the n-type mechanism of pure $MoSe_2$ to the p-type charge conduction in Nb-doped $MoSe_2$ [32]. In the present study, single crystals of WS_2 and $V_{0.25}W_{0.75}Se_2$ were grown by direct vapour transport technique [11,19]. Efforts have been made to study the photoresponse of the n-WS_2/p-$V_{0.25}W_{0.75}Se_2$ heterojunction diode fabricated by the layer transfer technique.

2. Experimental

In the present study, the direct vapour transport grown crystals of n-WS_2 and p-$V_{0.25}W_{0.75}Se_2$ were exfoliated by Scotch tape to provide a fresh unreacted surface with minimum defects. The fresh surface of the crystals was observed by using a Carl Zeiss optical microscope and micrographs of the crystal are displayed in

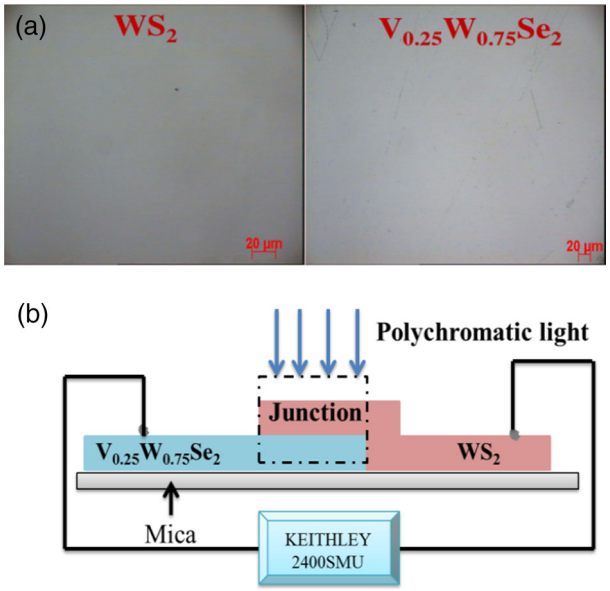

Figure 1. (**a**) Microstructure of exfoliated flakes of WS_2 and $V_{0.25}W_{0.75}Se_2$ crystals and (**b**) schematic diagram of the n-WS_2/p-$V_{0.25}W_{0.75}Se_2$ heterostructure.

figure 1a. The thicknesses of both exfoliated samples are measured to be about 2 μm. The cleaved crystal of WS_2 was then transferred on to the $V_{0.25}W_{0.75}Se_2$ substrate. The formed junction was then placed under low pressure for a few hours. The fabrication of the heterojunction interfaces was completed by making contacts with Ag paste. A schematic diagram of the heterojunction is shown in figure 1b. Determination of the electrical properties of the as-prepared devices started with the current–voltage characteristics at room temperature (Keithley 2400SMU); on confirmation of the rectifying behaviour of the heterojunction, the process was repeated for different intensities of light. The effect of bias voltage and illumination power on the photoresponse of the $WS_2/V_{0.25}W_{0.75}Se_2$ heterostructure is also investigated.

3. Results and discussion

Single crystals of WS_2 and $V_{0.25}W_{0.75}Se_2$ were grown by the direct vapour transport technique and were used for the fabrication of the device. The quality of the crystal is the most crucial part and it affects the performance of the device. The crystals grown by the direct vapour transport technique have remarkable features such as flat and shiny surface, uniform thickness, high surface-to-volume ratio, clean surface without any kind of impurity or dangling bond, etc. [19]. However, the growth by this technique is promoted by a screw dislocation mechanism and spirals are developed on the surface of the crystals, which limit the performance of the device [19]. Moreover, the problems of rapid growth and low saturation in the vapour phase arise during the growth and dendrites can be grown on the surface of the crystals [33]. Therefore, the grown crystals were analysed by using an optical microscope and crystals with clean and flat surface were selected for the fabrication of the device. The micrographs of the clean surface of the WS_2 and $V_{0.25}W_{0.75}Se_2$ crystals are shown in figure 1a. The bulk WS_2 crystal exhibits an n-type semiconducting nature with electrons being the majority charge carriers [11]. The p-type semiconducting nature of $V_{0.25}W_{0.75}Se_2$ crystals was confirmed by the hot probe technique. The selected samples, WS_2 and $V_{0.25}W_{0.75}Se_2$, have a hexagonal lattice structure with the $P6_3/mmc$ space group. The lattice constants of WS_2 are $a = b = 3.15$ Å and $c = 12.32$ Å [11] and those of $V_{0.25}W_{0.75}Se_2$ are $a = b = 3.29$ Å and $c = 12.94$ Å [19].

The current–voltage method is found to be the most widely used technique to study the characteristics of the fabricated device because it readily shows the nature of rectification of contacts under test. Figure 2a shows the current–voltage characteristics of the fabricated n-WS_2/p-$V_{0.25}W_{0.75}Se_2$ heterostructure both in the dark and upon illumination of different intensities ranging from 10 to 100 mW/cm^2. The I–V curves show the rectifying nature of the junction. Upon illumination, a rise in the forward current is observed due to the photo-induced carriers in the extended part of the thin flakes of WS_2 and $V_{0.25}W_{0.75}Se_2$ crystals. It is attributed to the good photoconducting behaviour of the samples. For low intensity of illumination, i.e. from 10 to 30 mW/cm^2, there is no significant change in reverse current. The possible reasons are: (i) due to the comparatively larger thickness of the top (WS_2) layer, the incident illumination may not penetrate effectively through the top layer and (ii) there is inefficient diffusion of charge carriers towards the junction and therefore, the rise in reverse current is not realised. For higher intensity, i.e. >90 mW/cm^2, a noticeable change in the reverse current is found. The enhanced reverse current may be due to the diffusion of photogenerated charge carriers from the extended part to the junction, which results in the narrowing of the depletion region. Therefore, the reverse current increases as the intensity of incident illumination increases.

Besides these, the turn-on voltage in the dark is 0.253 V which is slightly reduced on illumination of the diode due to the narrowing of the depletion region. This supports the above discussion on the enhanced reverse current. The turn-on voltages for different intensities are measured and presented in figure 3. The rectification ratio was calculated at ±1 V bias voltage and the

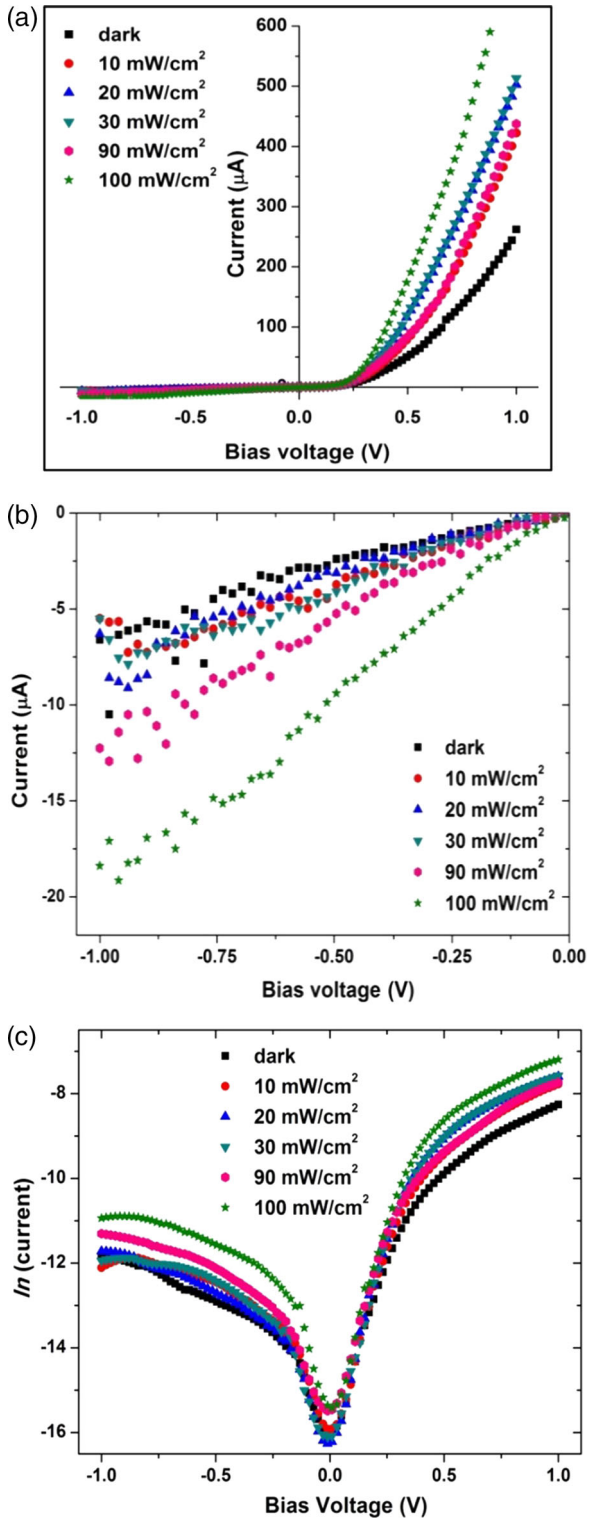

Figure 2. (**a**) I–V curves, (**b**) ln I–V curves and (**c**) ln I vs. ln V curve of the n-WS_2/p-$V_{0.25}W_{0.75}Se_2$ heterostructure.

estimated value is 39 under dark conditions. The plot of V vs. ln I is shown in figure 2b, which illustrates that the straight line in the lower forward bias region, i.e. 0–0.45 V [34], and the intercept on the y-axis of this straight

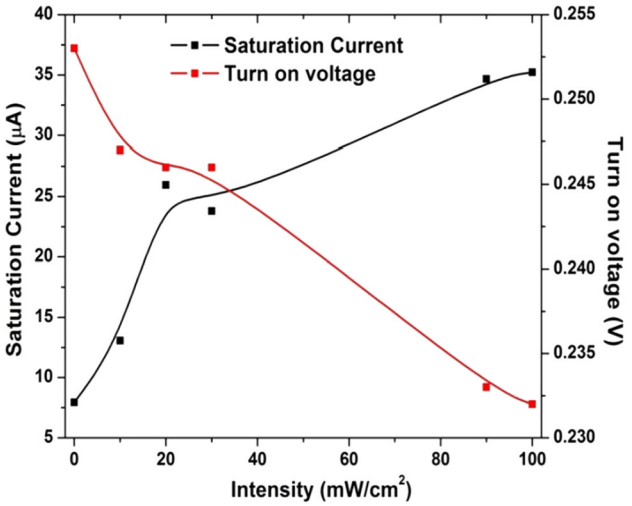

Figure 3. Variation of saturation current and turn-on voltage with the intensity of illumination for the n-WS_2/p-$V_{0.25}W_{0.75}Se_2$ heterostructure.

line give the value of the saturation current (I_0). The ideality factor (η) was also calculated from the slope of this straight line using the following relation based on the thermionic emission model:

$$\eta = \frac{q}{kT}\frac{\mathrm{d}V}{\mathrm{d}\,(\ln I)} = \frac{q}{kT} \times \frac{1}{\text{slope}}, \tag{1}$$

where q is the charge of the electron, k is the Boltzmann constant and T is the temperature.

The value of ideality factor of the fabricated heterojunction is ∼2. The ideality factor is simply a manifestation of the barrier uniformity and its higher value indicates the inhomogeneous junction [21]. This is due to the slight mismatch in the lattice of both the contacting materials which introduce interfacial strain across the junction. At the same time, the process-induced defects due to the tearing off of the layers when transferring them over one another also leaves broken layers across the junction from both the materials. These defect states play an important role in the overall charge transport across the interface [35]. Moreover, the possibility of generation of the third phase or the insulating layer at the interface is ruled out as these are chemically/environmentally stable compounds because of the d–d transition of electrons. The saturation current was evaluated for different intensities and presented in figure 3. The saturation current is found to increase upon illumination of the junction.

On detailed analysis, it is observed that the variation of current and voltage depicts linear region in the lower forward bias region from 0 to 0.11 V and exhibits the dominating mechanism of charge transport of Ohmic nature. The current in this region is mainly due to the generation recombination in the depletion region [36].

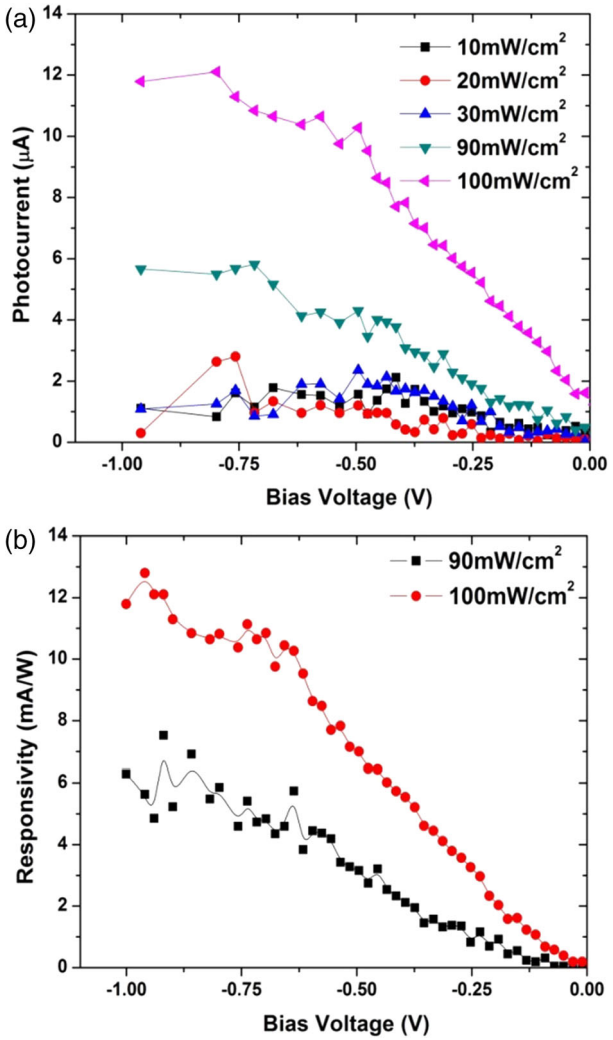

Figure 4. (**a**) Photocurrent and (**b**) responsivity with a reverse bias voltage for the n-WS_2/p-$V_{0.25}W_{0.75}Se_2$ heterostructure.

At slightly higher bias voltages from 0.13 to 0.3 V, the forward current increases exponentially with a voltage which is attributed to the thermionic emission of charge carriers. The I–V characteristic follows a power law $I \sim V^2$ in the higher voltage region from 0.68 to 1 V, which is generally attributed to a space-charge-limited current conduction for single-carrier injection behaviour [11].

As illustrated in figure 4a, the photocurrent generated upon illumination of the p–n junction is calculated under reverse bias condition. The photocurrent is found to be increased by increasing the bias voltage as well as power intensity of incident illumination. Besides this, the photoresponsivity of the fabricated heterojunction was also determined using the following relation:

$$R = \frac{I_{\text{ill}} - I_{\text{dark}}}{P_{\text{inc}}}, \tag{2}$$

where I_{ill} is the current under the illuminated condition, I_{dark} is the current in the dark and P_{inc} is the power of the incident light. The responsivity is plotted against bias voltage and presented in figure 4b. The responsivity is found to be enhanced upon increasing the bias voltage and illumination intensity.

4. Conclusions

The $WS_2/V_{0.25}W_{0.75}Se_2$ heterojunction is fabricated from the multilayer flakes of WS_2 and $V_{0.25}W_{0.75}Se_2$ crystals by the relatively simple layer transfer technique. The fabricated junction is then examined by the current–voltage technique. The ideality factor of the prepared junction is estimated to be ∼2 and its higher value suggests the inhomogeneity across the heterointerface at the junction. The rise in reverse current is realised at a higher intensity of illumination and the typical photodiode parameters such as photocurrent and responsivity are calculated at different bias and intensity of illumination.

References

[1] S Chuang, R Kapadia, H Fang, T C Chang, W C Yen, Y L Chueh and A Javey, *Appl. Phys. Lett.* **102**, 242101 (2013)
[2] H T Yuan, M S Bahramy, K Morimoto, S F Wu, K Nomura, B J Yang, H Shimotani, R Suzuki, M Toh and C Kloc, *Nat. Phys.* **9**, 563 (2013)
[3] A M Jones, H Y Yu, N J Ghimire, S F Wu, G Aivazian, J S Ross, B Zhao, J Q Yan, D G Mandrus and D Xiao, *Nat. Nanotechnol.* **8**, 634 (2013)
[4] A M Jones, H Yu, J S Ross, P Klement, N J Ghimire, J Yan, D G Mandrus, W Yao and X Xu, *Nat. Phys.* **10**, 130 (2014)
[5] K F Mak, C Lee, J Hone, J Shan and T F Heinz, *Phys. Rev. Lett.* **105**, 136805 (2010)
[6] S Zheng, L Sun, T Yin, A M Dubrovkin, F Liu, Z Liu, Z X Shen and H J Fan, *Appl. Phys. Lett.* **106**, 063113 (2015)
[7] M M Furchi, A Pospischil, F Libisch, J Burgdorfer and T Mueller, *Nano Lett.* **14**, 4785 (2014)
[8] B W H Baugher, H O H Churchill, Y Yang and P Jarillo-Herrero, *Nat. Nanotechnol.* **9**, 262 (2014)
[9] A Pospischil, M M Furchi and T Mueller, *Nat. Nanotechnol.* **9**, 257 (2014)
[10] C U Vyas, P Pataniya, C K Zankat, V M Pathak, K D Patel and G K Solanki, *Mater. Sci. Semicond. Process.* **71**, 226 (2017)
[11] S Kapatel, C K Sumesh, P Pataniya, G K Solanki and K D Patel, *Eur. Phys. J. Plus* **132**, 191 (2017)
[12] R H Friend and A D Yoffe, *Adv. Phys.* **36**, 1 (1987)
[13] Q H Wang, K Kalantar-Zadeh, A Kis, J N Coleman and M S Strano, *Nat. Nanotechnol.* **7**, 699 (2012)

[14] M Chhowalla, H S Shin, G Eda, L J Li, K P Loh and H Zhang, *Nat. Chem.* **5**, 263 (2013)
[15] D Jariwala, V K Sangwan, L J Lauhon, T J Marks and M C Hersam, *ACS Nano* **8**, 1102 (2014)
[16] H Zeng, *Sci. Rep.* **3**, 1608 (2013)
[17] W J Zhao, Z Ghorannevis, L Q Chu, M L Toh, C Kloc, P H Tan and G Eda, *ACS Nano* **7**, 791 (2013)
[18] W S Yun, S W Han, S C Hong, I G Kim and J D Lee, *Phy. Rev. B* **85**, 033305 (2012)
[19] G K Solanki, P Pataniya, C K Sumesh, K D Patel and V M Pathak, *J. Crystal Growth* **441**, 101 (2016)
[20] S Y Hu, M C Cheng, K K Tiong and Y S Huang, *J. Phys.: Condens. Matter* **17**, 3575 (2005)
[21] M R Laskar, D N Nath, L Ma, E W Lee II, C H Lee, T Kent, Z Yang, R Mishra, M A Roldan, J-C Idrobo, S T Pantelides, S J Pennycook, R C Myers, Y Wu and S Rajan, *Appl. Phys. Lett.* **104**, 092104 (2014)
[22] C-H Chen, C-L Wu, J Pu, M-H Chiu, P Kumar, T Takenobu and L-J Li, *2D Mater.* **1**, 034001 (2014)
[23] M P Deshpande, J B Patel, N N Pandya, M N Parmar and G K Solanki, *Mater. Chem. Phys.,* **117**, 350 (2009)
[24] L J Li, Y P Sun, X D Zhu, B S Wang, X B Zhu, Z R Yang and W H Song, *Solid State Commun.* **150**, 2248 (2010)
[25] Z Huang, T Wu, S Kong, Q-L Meng, W Zhuang, P Jiang and X Bao, *J. Mater. Chem. A* **4**, 10159 (2016)
[26] M Bougouma, B Guel, T Segato, J B. Legma and M-P Delplancke Ogletree, *Bull. Chem. Soc. Ethiop.* **22**(**2**), 225 (2008)
[27] Z Ma, K M Yu, L Liu, L Wang, D L Perry, W Walukiewicz, P Yu and S S Mao, *Appl. Phys. Lett.* **91**, 092113 (2007)
[28] J M Xu, L Li, S Wang, H L Ding, Y X Zhang and G H Li, *Cryst. Eng. Commun.* **15**, 3296 (2013)
[29] P Desai, D D Patel and A R Jani, *Mater. Sci. Semicond. Process.* **24**, 40 (2014)
[30] T Manago, S Ishida, H Geka and I Shibasaki, *J. Appl. Phys.* **117**, 065701 (2015)
[31] X Sun, J Dai, Y Guo, C Wu, F Hu, J Zhao, X Zeng and Y Xiea, *Nanoscale* **6**, 8359 (2014)
[32] Y Jin, D H Keum, S J An, J Kim, H S Lee and Y H Lee, *Adv. Mater.* **27**, 5534 (2015)
[33] P Pataniya, G K Solanki, K D Patel, V M Pathak and C K Sumesh, *Mater. Res. Express* **4**, 106306 (2017)
[34] S M Sze, *Physics of semiconductor devices* (Wiley-Interscience, New York, 1969)
[35] E H Rhoderick and R H Williams, Metal–semiconductor contacts, in: *Monographs in electrical and electronic engineering* (Oxford Science Publications, Clarendon Press, New York, 1988) Vol. 19
[36] N Koteeswara Reddy, Q Ahsanulhaq, J H Kim and Y Hahn, *Appl. Phys. Lett.* **92**, 043127 (2008)